JCTC Journal of Chemical Theory and Computation

Article

pubs.acs.org/JCTC

Effects of Molecular Dynamics Thermostats on Descriptions of Chemical Nonequilibrium

Alister J. Page,[†] Tetsushi Isomoto,[†] Jan M. Knaup,[‡,§] Stephan Irle,*[,∥] and Keiji Morokuma*[,†,⊥]

[†]Fukui Institute for Fundamental Chemistry, Kyoto University, Kyoto 606-8103, Japan

[‡]Department of Physics, Harvard University, Cambridge, Masachusetts 02138, United States

[§]Bremen Center for Computational Materials Science - BCCMS, University of Bremen, 28359 Bremen, Germany

[∥]Department of Chemistry, Graduate School of Science, Nagoya University, Nagoya 464-4602, Japan

[⊥]Cherry L. Emerson Center for Scientific Computation and Department of Chemistry, Emory University, Atlanta, Georgia 30322, United States

Supporting Information

ABSTRACT: The performance of popular molecular dynamics (MD) thermostat algorithms in constant temperature simulations of equilibrium systems is well-known. This is not the case, however, in the context of nonequilibrium chemical systems, such as chemical reactions or nanoscale self-assembly processes. In this work, we investigate the effect of popular thermostat algorithms on the "natural" (i.e., Hamiltonian) dynamics of a nonequilibrium, chemically reacting system. By comparing constant-temperature quantum mechanical MD (QM/MD) simulations of carbon vapor condensation using velocity scaling, Berendsen, Andersen, Langevin, and Nosé-Hoover chain thermostat algorithms with natural *NVE* simulations, we show that efficient temperature control and reliable reaction dynamics are mutually exclusive in such a system. This problem may be circumvented, however, by placing the reactive system in an inert He atmosphere, which is itself described using *NVT* MD. We demonstrate that both realistic temperature control and dynamics consistent with natural *NVE* dynamics can then be obtained simultaneously. In essence, the thermal energy created by the natural dynamics of the *NVE* subsystem is drained by the thermostat acting on the *NVT* atmosphere, without adversely affecting the dynamics of the reactive system itself.

INTRODUCTION

Few computer simulation techniques developed in the 20th century have made an impact as significant and lasting as molecular dynamics (MD). Since the initial report of this technique in the 1950s by Alder and Wainwright[1,2] and Rahman,[3] MD has become an invaluable tool in the simulation of matter and its dynamics over temporal and spatial scales ranging from mesoscale phenomena,[4] down to elementary chemical processes at the molecular level.[5] Ongoing development aimed at increasing the spatial and temporal scales amenable to MD-based investigation (for example, MD in conjunction with course-grained approaches,[4,6] advanced configurational sampling,[7] and graphical processing units[8]) increases the appeal and applicability of MD still further.

MD in its original formulation results in the microcanonical "*NVE*" ensemble, viz. one in which the number of particles N, the volume V, and the total energy E of the system remain unchanged over time. The first successful attempt at correctly generating other ensembles during MD simulations (notably the *NVT* ensemble, where the simulation temperature T remains constant, at the expense of constant energy E) was made by Andersen in his seminal 1980 paper.[9] Beforehand, temperature control in MD simulations was obtained *via* scaling the particle velocities in an *ad hoc* manner.[10] Another pre-1980 attempt at MD temperature control was the advent of Langevin dynamics,[11,12] in which particles undergo collisions with a "heat bath", the latter of which is described by a friction coefficient and a stochastic force added to the classical equations of motion. Such dynamics yield a canonical distribution, but no conserved quantity. Moreover, this method yields unreliable dynamics with large friction coefficients. Andersen[9] also achieved the *NVT* ensemble using a stochastic heat bath, instead by periodically redrawing the velocities of randomly chosen particles from a Maxwell−Boltzmann (MB) distribution according to a certain probability. Andersen's thermostat correctly generates the *NVT* ensemble. Somewhat ironically, the thermostat reported in 1984 by Berendsen et al.[13] is more popular, despite the fact that it follows no well-defined ensemble (except, for large values of the Berendsen coupling-constant τ_T, one can obtain the microcanonical ensemble) and may lead to pathalogical problems (such as the "flying-ice-cube effect"[14]). More reliable are the extended Lagrangian dynamics proposed by Nosé[15] (which were subsequently refined by Hoover[16]), which yield the correct canonical ensemble. These dynamics can, however, give rise to nonergodic behavior. A solution to this problem of ergodicity was provided by Martyna et al.,[17,18] who proposed so-called Nosé−Hoover chains (NHCs), whereby each thermostat is coupled to one or more additional thermostats. Despite more recent developments in MD thermostat algorithms (such as the generalized stochastic methods of Bussi et al.,[19−21] and the extension to the Berendsen approach of Eslami et al.[22]), we will restrict our discussion in the present work to the velocity scaling, Langevin,

Received: June 5, 2012

dx.doi.org/10.1021/ct3004639 | J. Chem. Theory Comput. XXXX, XXX, XXX−XXX

Andersen, Berendsen, and NHC approaches, i.e., those that are most commonly used at the present time.

As alluded to above, the performance of these popular themostats regarding equilibrium systems is well-established. The same may be said regarding the numerical parameters necessary to obtain good performance (whether it be heuristically known or based upon more fundamental physical considerations). It is generally well-known that stochastic thermostats destroy "true" *NVE* dynamics (i.e., Hamiltonian dynamics) in equilibrium systems, and that one should not use them to compute dynamic properties.[23,24] On the other hand, less is known regarding the relationship between nonequilibrium dynamics and popular thermostat algorithms. Of primary interest to us are systems in a state of chemical nonequilibrium, such as chemical reactions and emergent phenomena, for instance self-assembly processes. Despite vast literature concerning systems in other forms of nonequilibrium (such as heat/mass transfer and molecular diffusion/transport[25−27]), and in the context of other physical phenomena (such as the structural evolution of proteins and macromolecules[28−30]), no systematic investigation into the effects of thermostats on nonequilibrium chemical reaction dynamics has come to our attention. In order to perform such an investigation, one must first address the more fundamental issue of what distribution of particle velocities (i.e., ensemble), $P(v)$, defines a nonequilibrium chemical system, knowing *a priori* that it is not Maxwellian in nature (see below). One must assume that no "general" nonequilibrium ensemble exists; rather, particular dynamics/ensembles typify particular classes of nonequilibrium systems. Thus, the disruption of the "natural" Hamiltonian dynamics by a particular thermostat algorithm may be increased for particular types of nonequilibrium systems and decreased for others.

We aim to address this shortcoming in the present work in the context of MD simulations of self-assembly phenomena. We focus on carbon vapor condensation—the initial stage of fullerene formation—which we take to be an archetypal nonequilibrium system (an assumption that is not without physical basis, considering the similarity of this process with the growth of other carbon nanostructures, such as carbon nanotubes[31] and graphene[32]). Quantum mechanical MD (QM/MD) simulations of carbon condensation have been reported by our group on a number of previous occasions.[33,34] The mechanism of fullerene self-assembly is therefore well established. Driven by the spontaneous reaction of an ensemble of C_2 moieties (generated *via* carbon-arc discharge[35] or laser-evaporation of graphite[36]) at high temperatures (typically on the order of 1000−2000 K), initially these C_2 species undergo barrierless, highly exothermic addition reactions which result first in extended C_n chains. These in turn coalesce, providing a "Y-junction" precursor from which polygonal rings (and ultimately closed-cage structures) form. In this work, we focus on the precise nature of the natural, *NVE* dynamics of this self-assembly process and how these dynamics can best be approximated using popular thermostat algorithms while controlling the environmental temperature at a physically realistic level. We will also compare these thermostat algorithms with a novel temperature control method, in which temperature is controlled despite the absence of a thermostat acting directly on the reactive subsystem.

COMPUTATIONAL DETAILS

Quantum Chemical Methodology. The MD method employed here involved the integration of the classical equations of motion using the velocity-Verlet algorithm[37] with a time-step Δt = 1 fs. All QM/MD simulations reported in this work are 100 ps in length. We note here, however, that much of the analysis that follows focuses on the initial 10 ps of simulation (the period during which the system is furthest from chemical/thermal equilibrium). At each step of the MD simulation, QM energy and gradients were evaluated "on-the-fly" using the self-consistent charge density-functional tight-binding (DFTB) method.[38] DFTB parameters from the mio-0-1 parameter set[38] were employed throughout this work for C−C interactions. A finite electronic temperature, $T_e = T_n$ = 1200 K, was employed in all QM/MD simulations reported in this work. The occupancies of molecular orbitals in the vicinity of the Fermi-level therefore varied continuously over the interval [0:2]. He−He and He−C interactions used a Lennard-Jones potential in conjunction with parameters from ref 39.

We consider both *NVE* and *NVT* QM/MD simulations in this work; all *NVT* MD simulations employed thermostat routines that were implemented "in-house". Thermostats considered here include ad hoc velocity-scaling, Langevin, Andersen, Berendsen, and NHC (chain-length, M = 3) methods. The validity of these thermostat algorithms has been ensured *via* QM/MD simulations of nonreactive N_2 ensembles. We relegate all further discussion of these equilibrium QM/MD simulations to Supporting Information considering our present aim, suffice it to say that each thermostat algorithm has been validated.

Model Nonequilibrium Chemical System and Methods of Temperature Control. The nonequilibrium chemical system employed in this work consisted of 30 C_2 moieties distributed randomly throughout a 3 × 3 × 3 nm box (see Figure 1a). We note that this density (6.7 carbon atoms/nm^3) is on the same order as that employed in experimental fullerene synthesis[40] (*c.a.* 0.1−1.0 carbon atoms/nm^3). Periodic boundary conditions were enforced on all QM/MD trajectories, using a 1 × 1 × 1 k-point sampling scheme. A total of 10 statistically independent trajectories were computed for each combination of thermostat and corresponding coupling strength (Table 1). For each thermostat, we employ coupling strengths varying over several orders of magnitude. This resulted in a total of 340 *NVT* QM/MD simulations of C_2 condensation (and an additional 300 benchmark N_2 trajectories; see Table S1 in Supporting Information for coupling strengths of N_2 *NVT* MD simulations). Initial velocities of all atoms were drawn from a MB distribution at 1200 K; the target temperature of each *NVT* MD trajectory was then set to 1200 K throughout the remainder of the simulation.

In addition to *NVT* MD temperature control, we have considered an alternative approach, so-called "natural" temperature control of the nonequilibrium C_2 system, that is, temperature control in the absence of a thermostat. This has been achieved by placing the reactive C_2 system in He atmospheres of varying densities (60 and 120 He atoms, giving a C/He ratio of 1:1 and 1:2, respectively, see Figure 1b). We consider two alternative 'natural' temperature control approaches here that are related to recent fullerene formation simulations in our own group[41] and others.[42−44] First, we simply define the initial velocities of the surrounding He atoms using a MB distribution at 1200 K, after which we run *NVE*

dx.doi.org/10.1021/ct3004639 | J. Chem. Theory Comput. XXXX, XXX, XXX−XXX

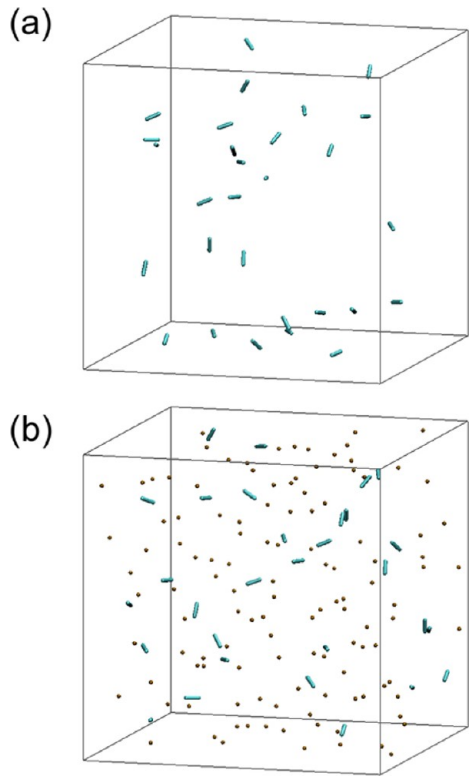

Figure 1. An archetypal chemical nonequilibrium system: initial random ensembles of 30 C_2 (a) without and (b) with a He atmosphere (120 He atoms in the case of b). The boxes denote the boundaries of the 3 × 3 × 3 supercell.

Table 1. Thermostats and Thermostat Coupling Strengths (ps^{-1}) Employed in *NVT* QM/MD Simulations of the Reactive C_2 Ensemble

vel. scaling (ν)	Andersen (ν)	Berendsen (τ_T)	Langevin (Γ)	Nosé-Hoover chain (ω)
1.0×10^{-3}	1	5×10^{-3}	0.1	0.19
1.0×10^{-2}	10	5×10^{-2}	1	9.4
5.0×10^{-2}	25	0.1	10	18.8
0.2	50	0.5	80	94.2
0.5	100	1.0	150	188.4
1.0	150	5.0	500	
5.0				

MD on the combined C/He system in the manner of Peng et al.[43] As we will show in the following discussion, this method is, not unexpectedly, unsuccessful at maintaining a realistic temperature even over short time scales, due to the high exothermicity of the condensation process. Our second approach involves partitioning the combined C/He system into C-only and He-only parts, in a similar fashion to Xi-Jing and co-workers.[42,44] The initial velocities of these subsystems are then defined using MB distributions at 1200 K. The combined C/He system is then forced into a two-component canonical ensemble of states, by enforcing NHC dynamics (*via* an NHC $M = 3$ thermostat, $T_n = 1200$ K) only on the He-only subsystem. In effect, we believe this partitioning of the C/He system to be a realistic approximation to the situation observed in reality. Fullerene synthesis (for example *via* carbon-arc discharge[35] or laser-evaporation of graphite[36]) typically takes place in an inert atmosphere of He or Ar buffer gas. Thus, the natural increase in temperature caused by repeated exothermic C−C bond formation reactions is removed by the continual arrival of new, cooler He/Ar atoms. Despite the similarity between this approach and previous simulations,[42,44] we expect that the partitioning approach presented here (in which a 1200 K NHC thermostat is applied to the He-only subsystem) to be more efficient at maintaining a realistic simulation temperature with respect to experimental conditions. This is due to two considerations: we are enforcing a lower temperature on the He-only subsystem (1200 K versus 2000 K[42,44]); and the NHC thermostat is applied at each MD iteration (whereas previously[42,44] each He atom's velocity was rescaled only when it exceeded 2500 K).

There are few examples of such two-component partitioning of a chemically reactive nonequilibrium MD simulation, as noted above. However, partitioning MD simulations with multiple thermostats and using explicit solvents is a standard approach in the context of simulating biological and macromolecules with MD (see refs 29, 30, and 45 and references therein). Lingenheil et al.[29] recently investigated in detail the effects of such partitioning on the infamous "hot-solvent/cold-solute" problem[28,46] in this context. By coupling different thermostats to a solute/solvent system—or, in the most noninvasive approach, allowing the solute subsystem to be described simply *via* Newtonian dynamics with no thermostat whatsoever—Lingenheil et al. aimed to provide a homogeneous temperature distribution over the entire system, while simultaneously generating the correct statistical ensemble in the solute subsystem. Our C/*NVT*(He) approach here is equivalent to this most noninvasive approach of Lingenheil et al., with the reactive C_2 subsystem ("solute") being described using Newtonian dynamics and the inert He atmosphere ("solvent") being kept at a constant temperature *via* an external thermostat algorithm. Nevertheless, our aim is somewhat different. We are interested only in maintaining a realistic simulation temperature for the whole system, since the C_2 (solute) subsystem is not at chemical or thermal equilibrium and so need not define a canonical ensemble.

As noted above, fullerene formation from small carbon fragments starts with the formation of short polyyne chains, which later coalesce to form polygonal carbon rings. Populations of short C_n species therefore serve as convenient indicators of the dynamics of the fullerene formation process in its initial stages. Our discussion of the performance of the various thermostats studied here will therefore center on the comparison of C_n populations obtained *via* natural, *NVE* dynamics (both with and without a He atmosphere) and those obtained using each thermostat algorithm. Similarly, the distribution of nuclear velocities, $P(v)$, obtained from these *NVE* and *NVT* simulations will also be compared toward this end.

RESULTS AND DISCUSSION

"Natural" Dynamics of a Nonequilibrium Reactive System. We begin by discussing the natural *NVE* dynamics of the reactive C_2 system. The temperature and the evolution of C_n fragment populations during the first 10 ps of these simulations are shown in Figures 2a and 3a. Figure 3a shows that during this 10 ps period the reaction dynamics of the C_2 system are characterized by a sharp drop in the density of C_2 itself, which reacts to form primarily C_3, C_4, and C_5 moieties (i.e., short polyyne chains). Longer chains are also present, but not at particularly high concentrations. Ideally, an analysis of a longer MD simulation should be made here; however, Figure

dx.doi.org/10.1021/ct3004639 | J. Chem. Theory Comput. XXXX, XXX, XXX−XXX

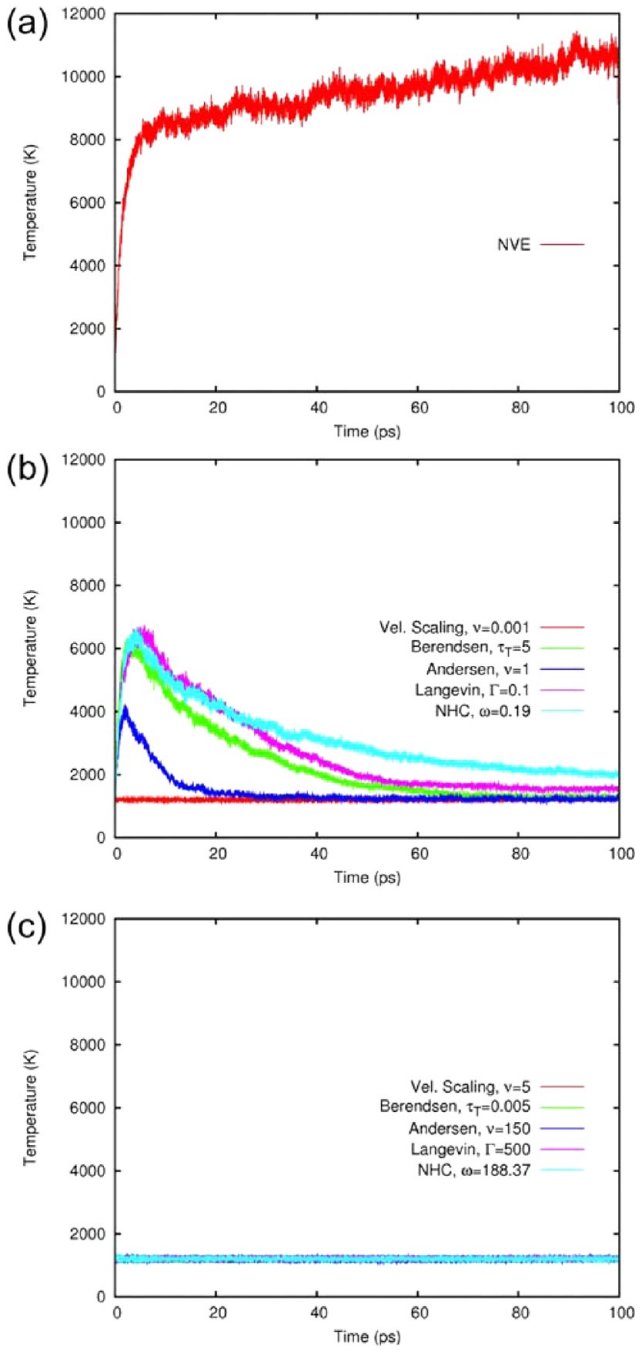

Figure 2. Simulation temperatures of reactive C_2 systems using (a) *NVE* and (b,c) *NVT* MD with thermostats coupled (b) weakly and (c) strongly to the degrees of freedom of the system. All data averaged over 10 trajectories; coupling strengths given in ps^{-1}.

2a shows that the *NVE* simulation temperature exceeds 6000 K prior to 10 ps. This is an entirely unrealistic situation in relation to experimental results (but is the direct consequence of repeated exothermic C_2 addition reactions in an *NVE* ensemble). Such a high temperature corresponds to a tendency toward a state of maximized entropy in the system that eventually equilibrates at over 10 000 K. The system in this state consists essentially of high-energy C_3 and C_2 fragments. Clearly this is contrary to the situation in reality, in which fullerene cages are ultimately formed *via* the interaction of small C_n fragments at a constant temperature (yielding a lower-entropy system). We note that the early stages of carbon plasma condensation in a vacuum indeed feature the formation (in chronological order) of C, C_2, and C_3.[47]

The natural reaction dynamics of the *NVT* C_2 system are elucidated further in Figure 4a, in which the time-dependent C_2 $P(v)$ (cumulative atomic velocity distribution) of the *NVE*(C) simulation is detailed. The difference between this $P(v)$ distribution and the MB $P(v)$ is of particular interest here and underlines in essence a fundamental difference between nonequilibrium and equilibrium dynamics. That is, that $P(v)$ for a nonequilibrium system *cannot* resemble a MB $P(v)$ distribution at the same temperature. It is conceded, however, that there are several factors that determine how different equilibrium and nonequilibrium $P(v)$ distributions are, most notably, the nature of the nonequilibrium system itself. Furthermore, environmental factors such as temperature, phase, and density also contribute in this respect. The nonequilibrium system of concern here is thus a somewhat extreme example of this point—of particular note is the large fraction of carbon atoms with velocities smaller than the mean velocity of the time-dependent MB distribution in the first 10 ps of reaction ("cold" carbon).

Effects of Molecular Dynamics Thermostats on Nonequilibrium Chemical Dynamics. The most obvious solution to the temperature issues raised in the preceding section is simply to enforce some kind of thermostat algorithm on the degrees of freedom of the system, thereby bringing the simulation temperature back under control. However, this necessarily impacts the natural dynamics of the chemical system, as we will discuss momentarily. We will focus here primarily on the NHC thermostat, since it typifies the general relationship observed between a thermostat's coupling strength and the dynamics obtained for all thermostats considered. Data pertaining to other thermostats is provided in the Supporting Information.

Figure 2b and c show the effect of weak and strong coupling of all thermostats considered on the simulation temperature of the reactive C_2 system. Unsurprisingly, by increasing the coupling strength of each thermostat, tighter control over the simulation temperature is obtained. In particular, tighter control over the simulation temperature in the first 10 ps of simulation is obtained, to the point at which temperature control on the reacting system is essentially perfect using the strongest coupling constants considered here. It is noted that the physical meaning of the trajectories corresponding to Figure 2c is limited due to the excessive coupling strength; we include them here only for the sake of comparison. Comparison of the C_n populations obtained using an NHC thermostat (Figure 3b,c) with natural *NVE* populations (Figure 3a) reveals immediately the effect of a strongly coupled thermostat algorithm on dynamic phenomena. In this case, the populations of short C_n fragments are significantly different; most notable is the total absence of C_3 and C_5 moieties. The rate of consumption of C_2 is also noticeably decreased compared to that observed using weaker NHC coupling, and *NVE* itself. Cluster sizes obtained using the NHC thermostat (Figure 3c) also deviate substantially from those observed during *NVE* simulations, with almost all of the initial carbon density being incorporated into a single cluster within the first 10 ps. Equivalent (and in some cases, exaggerated) trends are evident also for the velocity-scaling stochastic thermostats considered in this work. For example, by weakly coupling the Berendsen and Langevin thermostats, reasonable agreement between these

dx.doi.org/10.1021/ct3004639 | J. Chem. Theory Comput. XXXX, XXX, XXX–XXX

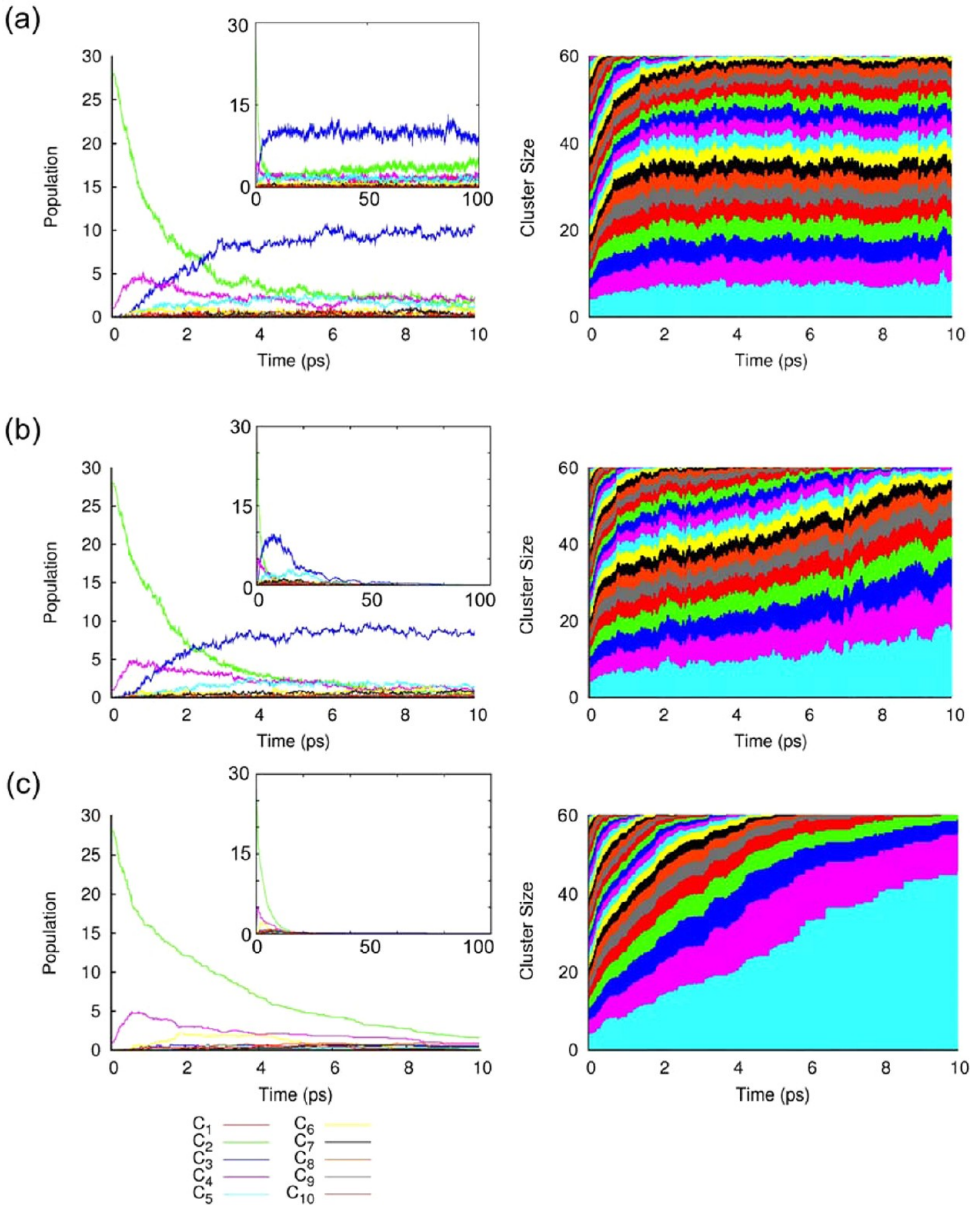

Figure 3. Comparison of C_n formation (left) and cluster size evolution (right) in a reactive C_2 system using (a) *NVE*(C) and a NHC thermostat coupled (b) weakly (ω = 0.19 ps^{-1}) and (c) strongly (ω = 188.37 ps^{-1}) to the degrees of freedom of the system. Comparison with Figure 2 shows that while weak coupling yields more accurate dynamics, temperature control is sacrificed, and vice versa. Cluster size evolutions show the size of each distinct carbon cluster at each MD iteration, and how these cluster sizes change over the course of the simulation. All data averaged over 10 trajectories.

NVT dynamics and natural *NVE* dynamics during the initial stages of reaction can be obtained; yet Figure 2 shows that temperature control during this period is minimal.

Figure 4 corroborates this relationship between a thermostat's coupling strength and the *NVT* reaction dynamics obtained. For instance, Figure 4b shows that in the first 10 ps of simulation the characteristic "cold" carbon peak observed in *NVE* simulations, described above, is also observed when the NHC thermostat is weakly coupled to the system. This is not so in the case of strong coupling, as shown in Figure 4c. As is expected, the latter $P(v)$ conforms more strictly to that of a MB distribution at 1200 K. This comparison highlights once again the dramatic effect brought about by strong coupling of a MD thermostat to a reactive chemical system. Indeed, results obtained here suggest that nonequilibrium dynamics are in fact more sensitive to the value of a thermostat's coupling parameter, compared to the dynamics of a comparable equilibrium system (see Supporting Information). Comparable results were also observed with other thermostats investigated here. For instance, *ad hoc* velocity scaling fails to reproduce the $P(v)$ observed in the *NVE*-based simulations discussed above, irrespective of the coupling strength employed. This is not unexpected, due to the construction of the algorithm itself; at each MD iteration, the nuclear velocities are scaled such that the simulation temperature is constantly equal to the "desired" temperature (1200 K in this case). Similarly, the $P(v)$ distribution obtained using the Andersen thermostat also adhered closely to a MB $P(v)$ distribution at 1200 K, even during the most reactive period of the simulation. This is also unsurprising, since, as noted in the Introduction, the Andersen

dx.doi.org/10.1021/ct3004639 | J. Chem. Theory Comput. XXXX, XXX, XXX−XXX

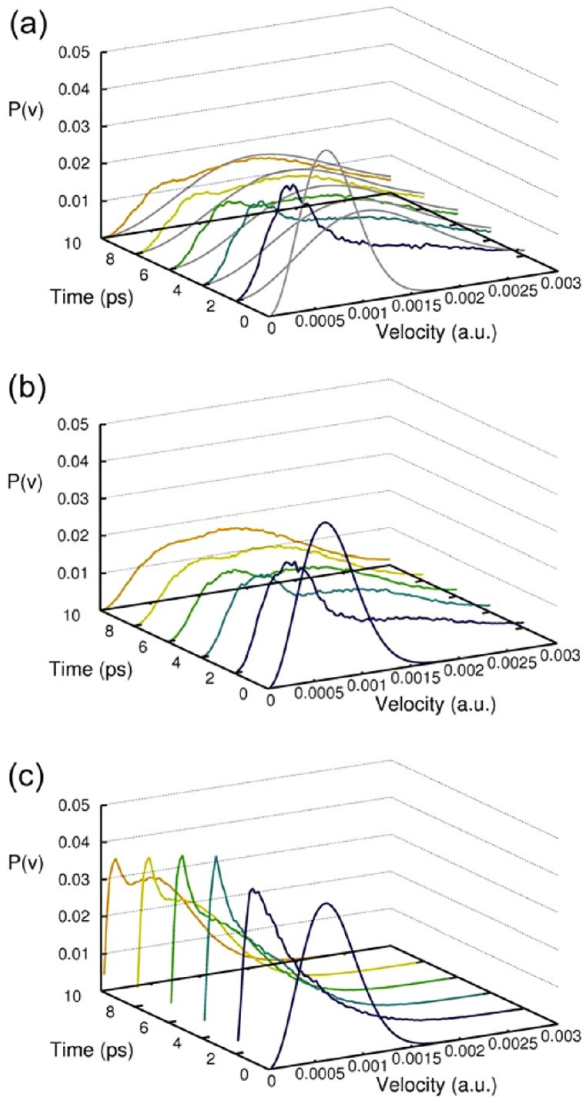

Figure 4. Comparison of time-dependent $P(v)$ for a reactive C_2 system using (a) *NVE*(C) and a NHC thermostat coupled (b) weakly (ω = 0.19 ps^{-1}) and (c) strongly (ω = 188.37 ps^{-1}) to the degrees of freedom of the system. For reference, time-dependent MB $P(v)$ distributions at the corresponding *NVE* MD simulation temperatures are included in part a (gray lines). All data averaged over 10 trajectories.

thermostat results in a correct *NVT* ensemble. Weakly coupled Berendsen and Langevin algorithms reproduce the distinctive "cold" carbon peak in $P(v)$ near 5×10^{-4} a.u.; however, once more this agreement comes at the expense of realistic temperature control.

Thus, a contradiction of sorts is revealed; in order for reasonable temperature control of such a chemical reaction to be achieved, any thermostat must be coupled tightly to the degrees of freedom of the system. Doing so, however, adversely affects the natural reaction dynamics that would otherwise be observed. It seems then that for such a reactive system, rigorous reaction dynamics and temperature control are mutually exclusive. One is forced to therefore achieve a balance in atomistic MD simulations of chemical reactions at constant temperature. That is, a balance between the thermostat (which forces the system toward equilibrium, thereby providing a constant simulation temperature) and the natural dynamics of the system (which force the system away from equilibrium and result in fluctuating simulation temperatures). However, as we will show in the following discussion, this contradiction seemingly applies only to "artificial", external thermostat algorithms that are coupled to the degrees of freedom of the system.

"Natural" Temperature Control in a Non-Equilibrium Chemical System. We turn now to address alternative ways in which the effects of an external thermostat algorithm on natural chemical reaction dynamics can be circumvented. As detailed above, our approach in this work involves the introduction of a He atmosphere.

Figure 5 compares the simulation temperatures observed in the reactive C_2 system using *NVE*(C), *NVE*(C/He), and C/*NVT*(He) simulations. The introduction of He atmospheres using C/He ratios of 1:1 and 1:2, with He dynamics described *via* the *NVE* ensemble, results ultimately in equilibrated temperatures of *ca.* 8000 and 6000 K, respectively. The He atmosphere is, to a limited extent, successful in draining off the thermal energy resulting from exothermic C−C bond formation. Unsurprisingly, however, much of it remains in the reactive C_2 subsystem. These temperatures are therefore still almost an order of magnitude too high with respect to experimental results. Upon the introduction of an *NVT* He atmosphere, however, the simulation temperature is dramatically reduced. In effect, the energy produced by the repeated exothermic C−C bond formation reactions is now continuously drained from the system by the thermostat acting on the He subsystem. However, the natural *NVE* dynamics of the C subsystem are not explicitly altered by this arrangement (as we will discuss at greater length below). Using a C/He ratio of 1:1, the C/*NVT*(He) simulation yielded an average simulation temperature no higher than *ca.* 3600 K, which was ultimately reduced to 1200 K by 100 ps (i.e., the temperature enforced on the He subsystem). This decrease is due to the decreasing frequency of C−C bond formation, which equates to the chemical equilibration of the system. Upon increasing the He density, this maximum temperature was reduced to *ca.* 2000 K, one that is in line with experimental temperatures. The

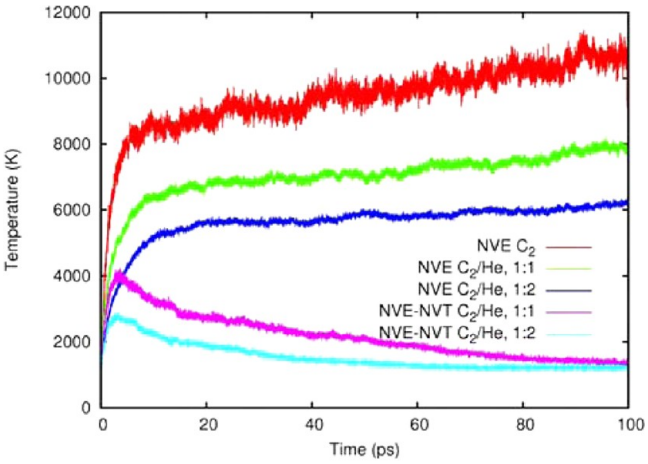

Figure 5. Simulation temperatures of reactive C_2 and C/He systems using *NVE* MD. Natural *NVE* dynamics lead immediately to an unrealistically high temperature, representing the tendency toward a state of maximized entropy. "Natural" temperature control, in the form of *NVE* He and *NVT* He atmospheres, controls this increase in temperature to various degrees. All data averaged over 10 trajectories.

dx.doi.org/10.1021/ct3004639 | J. Chem. Theory Comput. XXXX, XXX, XXX−XXX

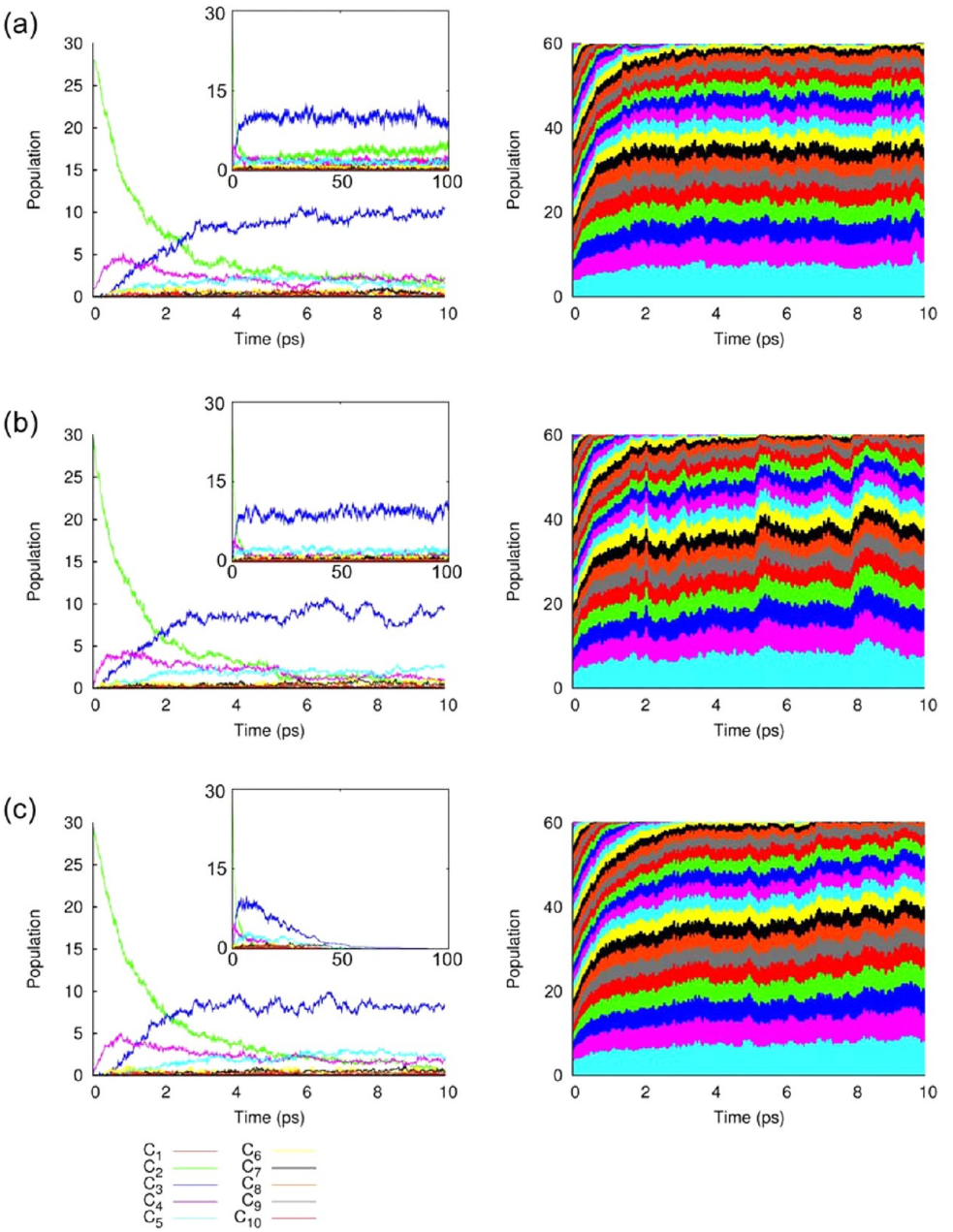

Figure 6. Comparison of C_n formation (left) and cluster size evolution (right) in a reactive C_2 system using (a) *NVE*(C), (b) *NVE*(C/He), and (c) C/*NVT*(He) simulations. *NVE*(C) and *NVE*(C/He) simulations fail to form larger clusters over 100 ps (inset), whereas the lower temperature C/*NVT*(He) simulations do not. All data averaged over 10 trajectories. *NVE*(C/He) and C/*NVT*(He) simulations use C/He = 1:1.

increased He density in this case also forced the simulation temperature to 1200 K at a faster rate, as one would expect.

Supplementary C/*NVT*(He) simulations of this system using a lower temperature for the inert He atmosphere (298 K) show that the reaction dynamics of the condensing carbon subsystem are remarkably invariant to the He temperature. The most notable difference observed when using this lower temperature He atmosphere is a higher initial peak in the system temperature. Using C/He ratios of 1:1 and 1:2, this reduction was *ca.* 500 and 700 K, respectively (from comparison of Figure 5 with Figure S1). The equilibrated temperature was also 298 K due to the decreased temperature of the He atmosphere, as one may expect. Otherwise, the effect of a colder He atmosphere on the dynamics of the reaction was effectively negligible, as can be seen from a comparison of Figure 6 and Figure 7 with Figure S2 and Figure S3, respectively.

Comparison of the temperature profiles observed in these C/*NVT*(He) simulations (Figure 5) with those observed in *NVT* simulation using a weakly coupled thermostat (Figure 2b) shows that the former method is more successful at minimizing the peak simulation temperature during this initial reactive period. The time required for each thermostat to remove this thermal energy from the system varies. In the case of a weakly coupled Andersen thermostat, the temperature is returned to 1200 K more efficiently than in the C/*NVT*(He) simulations. On the other hand, weakly coupled Berendsen, Langevin, and NHC thermostats return the temperature to 1200 K at a comparable rate to the C/*NVT*(He) simulations.

dx.doi.org/10.1021/ct3004639 | *J. Chem. Theory Comput.* XXXX, XXX, XXX–XXX

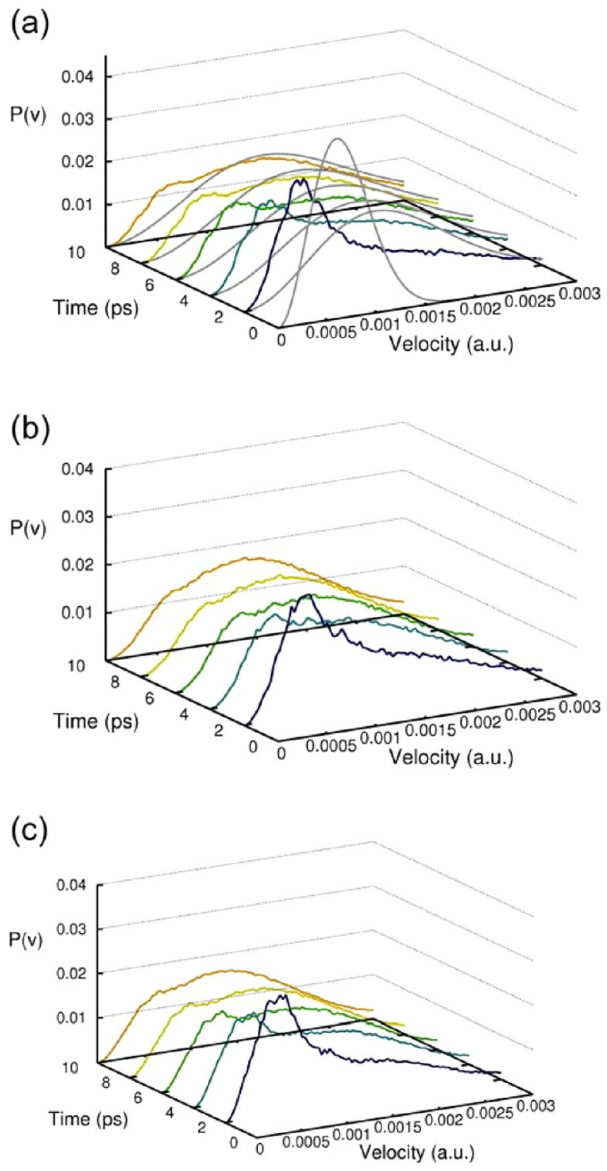

Figure 7. Comparison of time-dependent $P(v)$ of a reactive C_2 system using (a) *NVE*(C), (b) *NVE*(C/He), and (c) C/*NVT*(He) simulations. For reference, time-dependent MB $P(v)$ distributions at the corresponding *NVE* MD simulation temperatures are included in part a (gray lines). All data averaged over 10 trajectories. *NVE*(C/He) and C/*NVT*(He) simulations use C/He = 1:1. $P(v)$'s shown only take into account carbon atom velocities.

The introduction of a He atmosphere has the obvious additional effect that the mean free pathways of carbon molecular fragments are shortened, an effect that was speculated upon in the literature as a "caging effect".[41,48] This effect additionally reduces the energy production in reacting systems as it reduces the number of inelastic collisions. Unfortunately, both caging and temperature control/kinetic energy transfer effects of the He atmosphere are inseparably coupled, but we note that the caging effect should be small due to the much lighter mass of He in comparison to C.

We have demonstrated that temperature control can thus be achieved in a reactive *NVE* MD simulation without recourse to an artificial thermostat algorithm. However, it remains to show that, by doing so, the natural dynamics of the reactive process in question are not adversely affected. We address this point in Figures 6 and 7. These figures illustrate the effect of *NVE* He and *NVT* He atmospheres on the chemical products of the reactive C_2 system, and the evolution of the velocity distribution, $P(v)$, during the course of the reaction. Once again, we focus here only on the initial 10 ps of the fullerene formation process, since it is only this period in which physically relevant *NVE* dynamics are obtained. From the inset of Figure 6a, it is evident that after 100 ps (corresponding to a temperature of *ca.* 11 000 K, Figure 5), the initial C_2 system in the absence of He is converted into one essentially consisting of C_3 and C_2. The temperature is so high in this case that larger carbon fragments are thermodynamically unstable. This was also the case regarding the *NVE*(C/He) simulations (Figure 6b, inset), in which case the corresponding temperature at 100 ps was *ca.* 8000 K. On the other hand, the introduction of an *NVT* He atmosphere brought about a decrease in the populations of these short C_n fragments by *ca.* 50 ps (via their conversion into longer C_n chains and ultimately polygonal rings/fullerene cages), as mentioned in our previous work discussing the simulation of C_2 aggregation using Liouville−von Neumann dynamics.[49] We note here that, despite the continual C−C bond formation that must take place in order for this to occur, the simulation temperature never exceeded *ca.* 3600 K. Despite these differences between *NVE*(C), *NVE*(C/He), and C/*NVT*(He) simulations, Figure 7 shows that there is quantitative agreement regarding the populations of short polyyne chains, particularly C_2, C_3, C_4, and C_5, during the first 10 ps of the reaction. A comparison of Figure 3c and Figure 6c illustrates most succinctly the difference between C/*NVT*(He) and "artificial" temperature control, in terms of both the chemical products obtained and their structural composition (in terms of the carbon cluster sizes produced). Quantitative agreement between the $P(v)$ distributions of *NVE*(C), *NVE*(C/He), and C/*NVT*(He) simulations is also inferred from Figure 7. The *NVE*(C/He) and C/*NVT*(He) simulations produce $P(v)$ distributions that are in striking agreement with the natural *NVE*(C) dynamics. Most importantly, the prominent $P(v)$ peak at *ca.* 5×10^{-4} au is recovered, despite the presence of He in the system. The broadening of this shoulder as the system moves toward equilibrium is also recreated in these temperature-controlled simulations. Thus, not only has the simulation temperature been controlled but it has been done by enforcing an *NVT* ensemble on a nonreactive He subsystem. The dynamics of the reactive system of interest, the C_2 subsystem, are still described according to natural *NVE* dynamics. We note here however that the potential energies of neither the whole system nor the C_2 subsystem remain constant in such an arrangement.

CONCLUSION

We have presented a critical evaluation of the effect of popular MD thermostat algorithms (velocity scaling, Berendsen, Andersen, Langevin, and NHC) on the natural dynamics of a nonequilibrium, chemically reactive system. By comparing *NVT* simulations of a reactive C_2 system with natural *NVE* simulations, the relationship between these thermostats' coupling parameters and the reliability of the reactions dynamics produced has been revealed. In particular, reliable reaction dynamics and rigorous temperature control are apparently mutually exclusive in this case—reliable reaction dynamics of fullerene self-assembly were only obtained in *NVT* simulations where the thermostat was coupled weakly to the degrees of freedom of the system. In such a case, the coupling

dx.doi.org/10.1021/ct3004639 | J. Chem. Theory Comput. XXXX, XXX, XXX−XXX

was so weak that realistic temperature control was essentially sacrificed. On the other hand, by coupling the thermostat tightly to the system, temperature control was achieved at the expense of realistic reaction dynamics. Our work suggests that this is a contradiction inherent to any external thermostat algorithm. To this end, we have demonstrated a way in which this issue can be circumvented for carbon-condensation reactions, so-called "natural" temperature control in *NVE* MD simulations of fullerene self-assembly. By embedding the reactive C_2 system in an *NVT* He atmosphere, it was demonstrated that both realistic temperature control and dynamics consistent with natural *NVE* dynamics could be obtained simultaneously. In this case, the thermal energy created by repeated exothermic C−C bond formation was effectively drained from the C_2 subsystem by the thermostat acting on the He subsystem. The dynamics of the C_2 subsystem remained, however, explicitly unaffected by such an arrangement. Such a combined C/*NVT*(He) system more accurately approximates the situation in reality, since fullerene synthesis typically takes takes place in a cold, high pressure atmosphere of an inert gas (such as He or Ar). The presented method of "natural" temperature control is therefore highly specific to carbon-condensation reactions.

However, we believe that the results presented here have, in principle, much broader consequences in the context of MD simulations of nonequilibrium, chemically reactive systems. Our results demonstrate that realistic temperature control of a chemically reactive system requires more thought than simply applying an equilibrium thermostat algorithm to the system as a whole. All equilibrium thermostat algorithms describe specifically how the system in question is coupled to an external heat bath and ultimately amount to rescaling the velocities in some way. While such scaling may be suitable for an equilibrium system, it is too imprecise under nonequilibrium chemical conditions, such as those presented here. Conditions of chemical nonequilibrium instead require analysis of the physical manner in which thermal energy is dissipated from the system, and how efficiently such dissipation takes place. Only then can a model of heat dissipation be meaningful. As our results here demonstrate, it may be necessary to describe explicitly the heat dissipation from the reacting system to a heat bath (in this case a carrier gas). However, it may suffice to apply an equilibrium thermostat algorithm within the heat bath itself, since it is much closer to equilibrium than the reacting subsystem of interest. The way in which energy dissipates from a chemically reactive system will of course vary significantly between different systems. Temperature control of chemical nonequilibrium must therefore be carefully treated on a case-by-case basis.

■ ASSOCIATED CONTENT

Ⓢ Supporting Information

Details and thermostat coupling strengths of nonreactive N_2 *NVE*/*NVT* MD simulations; C_n population and $P(v)$ analysis for all reactive C_2 *NVT* MD simulations. This material is available free of charge via the Internet at http://pubs.acs.org.

■ AUTHOR INFORMATION

Corresponding Author

*E-mail: keiji.morokuma@emory.edu, sirle@chem.nagoya-u.ac.jp.

Notes

The authors declare no competing financial interest.

■ ACKNOWLEDGMENTS

The authors thank Prof. Shinji Saito, Institute for Molecular Science, Japan, for very helpful discussions. The authors would also like to thank Dr. Hu-Jun Qian, Jilin University, for providing C−He DFTB parameters. This work was in part supported by a CREST (Core Research for Evolutional Science and Technology) grant in the Area of High Performance Computing for Multiscale and Multiphysics Phenomena from the Japanese Science and Technology Agency (JST), and by a NINS (National Institutes of Natural Sciences) Program for Cross-Disciplinary Study. Computer simulations were performed using The Academic Center for Computing and Media Studies (ACCMS) at Kyoto University, and the Institute for Molecular Science (IMS) in Okazaki, Japan. A.J.P. acknowledges the Kyoto University Fukui Fellowship.

■ REFERENCES

(1) Alder, B. J.; Wainwright, T. E. *J. Chem. Phys.* **1957**, *27*, 1208−1209.
(2) Alder, B. J.; Wainwright, T. E. *J. Chem. Phys.* **1959**, *31*, 459−466.
(3) Rahman, A. *Phys. Rev.* **1964**, *136*, A405−A411.
(4) Merchant, B. A.; Madura, J. D. In *Ann. Rep. Comp. Chem.*; Elsevier: Amsterdam, 2011; Vol. *7*, pp 67−87.
(5) Jasper, A. W.; Nangia, S.; Zhu, C.; Truhlar, D. G. *Acc. Chem. Res.* **2006**, *39*, 101−108.
(6) Sherwood, P.; Brooks, B. R.; Sansom, M. S. *Curr. Opin. Struct. Biol.* **2008**, *18*, 630−640.
(7) Perez, D.; Uberuaga, B. P.; Shim, Y.; Amar, J. G.; Voter, A. F. In *Ann. Rep. Comput. Chem.*; Elsevier: Amsterdam, 2009; Vol. *5*, pp 79−98.
(8) Xu, D.; Williamson, M. J.; Walker, R. C. In *Ann. Rep. Comput. Chem.*; Elsevier: Amsterdam, 2010; Vol. *6*, pp 2−19.
(9) Andersen, H. C. *J. Chem. Phys.* **1980**, *72*, 2384−2393.
(10) Woodcock, L. V. *Chem. Phys. Lett.* **1971**, *10*, 257−261.
(11) Hiwatari, Y.; Stoll, E.; Schneider, T. *J. Chem. Phys.* **1978**, *68*, 3401−3404.
(12) Schneider, T.; Stoll, E. *Phys. Rev. B* **1978**, *17*, 1302−1322.
(13) Berendsen, H. J. C.; Postma, J. P. M.; van Gunsteren, W. F.; DiNola, A.; Haak, J. R. *J. Chem. Phys.* **1984**, *81*, 3684−3690.
(14) Harvey, S. C.; Tan, R. K.-Z.; Cheatham, T. E. *J. Comput. Chem.* **1998**, *19*, 726−740.
(15) Nosé, S. *J. Chem. Phys.* **1984**, *81*, 511−519.
(16) Hoover, W. G. *Phys. Rev. A* **1985**, *31*, 1695−1697.
(17) Martyna, G. J.; Klein, M. L.; Tuckerman, M. *J. Chem. Phys.* **1992**, *97*, 2635−2643.
(18) Martyna, G. J.; Tuckerman, M. E.; Tobias, D. J.; Klein, M. L. *Mol. Phys.* **1996**, *87*, 1117−1157.
(19) Bussi, G.; Donadio, D.; Parrinello, M. *J. Chem. Phys.* **2007**, *126*, 014101.
(20) Bussi, G.; Parrinello, M. *Comput. Phys. Commun.* **2008**, *179*, 26−29.
(21) Bussi, G.; Zykova-Timan, T.; Parrinello, M. *J. Chem. Phys.* **2009**, *130*, 074101.
(22) Eslami, H.; Mojahedi, F.; Moghadasi, J. *J. Chem. Phys.* **2010**, *133*, 084105.
(23) Frenkel, D.; Smit, B. *Understanding Mol. Simulation: From Algorithms to Applications*; Academic Press: San Diego, CA, 2002.
(24) Tanaka, H.; Nakanishi, K.; Watanabe, N. *J. Chem. Phys.* **1983**, *78*, 2626−2634.
(25) Dubbeldam, D.; Snurr, R. Q. *Mol. Simul.* **2007**, *33*, 305−325.
(26) Sarman, S.; Laaksonen, A. *J. Comput. Theor. Nanosci.* **2011**, *8*, 1081−1100.
(27) Sarman, S. S.; Evans, D. J.; Cummings, P. T. *Phys. Rep.* **1998**, *305*, 1−92.
(28) Cheng, A.; Merz, K. M. *J. Phys. Chem.* **1996**, *100*, 1927−1937.
(29) Lingenheil, M.; Denschlag, R.; Reichold, R.; Tavan, P. *J. Chem. Theory Comput.* **2008**, *4*, 1293−1306.

(30) Tobias, D. J.; Martyna, G. J.; Klein, M. L. *J. Phys. Chem.* **1993**, *97*, 12959−12966.
(31) Page, A. J.; Ohta, Y.; Irle, S.; Morokuma, K. *Acc. Chem. Res.* **2010**, *43*, 1375−1385.
(32) Wang, Y.; Page, A. J.; Nishimoto, Y.; Qian, H.-J.; Morokuma, K.; Irle, S. *J. Am. Chem. Soc.* **2011**, *133*, 18837−18842.
(33) Irle, S.; Page, A. J.; Biswajit, S.; Wang, Y.; Chandrakumar, K. R. S.; Nishimoto, Y.; Qian, H.-J.; Morokuma, K. In *Practical Aspects of Computational Chemistry II: An Overview of the Last Two Decades and Current Trends*; Springer-European Academy of Sciences: New York, 2012.
(34) Irle, S.; Zheng, G.; Wang, Z.; Morokuma, K. *J. Phys. Chem. B* **2006**, *110*, 14531−14545.
(35) Kratschmer, W.; Lamb, L. D.; Fostiropoulos, K.; Huffman, D. R. *Nature* **1990**, *347*, 354−358.
(36) Kroto, H. W.; Heath, J. R.; O'Brien, S. C.; Curl, R. F.; Smalley, R. E. *Nature* **1985**, *318*, 162−163.
(37) Swope, W. C.; Andersen, H. C.; Berens, P. H.; Wilson, K. R. *J. Chem. Phys.* **1982**, *76*, 637−649.
(38) Elstner, M.; Porezag, D.; Jungnickel, G.; Elsner, J.; Haugk, M.; Frauenheim, T.; Suhai, S.; Seifert, G. *Phys. Rev. B* **1998**, *58*, 7260−7268.
(39) Rappe, A. K.; Casewit, C. J.; Colwell, K. S.; Goddard, W. A.; Skiff, W. M. *J. Am. Chem. Soc.* **1992**, *114*, 10024−10035.
(40) Smalley, R. E. *Acc. Chem. Res.* **1992**, *25*, 98−105.
(41) Qian, H.-J.; Wang, Y.; Morokuma, K.; Irle, S. *Extended Abstract No. 823. Carbon* **2011**, Shanghai, China, July 25−29, 2011.
(42) Juan, G.; Zheng-Zhe, L.; Xi-Jing, N. *J. Chem. Phys.* **2007**, *126*, 174309.
(43) Peng, L.; Ning, X.-J. *J. Chem. Phys.* **2004**, *121*, 7701−7707.
(44) Yang, S.; Xi-Jing, N.; Peng, L. *J. Chem. Phys.* **2004**, *121*, 2013−2015.
(45) Fox, T.; Kollman, P. A. *Proteins* **1996**, *25*, 315−334.
(46) Oda, K.; Miyagawa, H.; Kitamura, K. *Mol. Simul.* **1996**, *16*, 167−177.
(47) Monchicourt, P. *Phys. Rev. Lett.* **1991**, *66*, 1430−1433.
(48) Wakabayashi, T.; Kasuya, D.; Shiromaru, H.; Suzuki, S.; Kikuchi, K.; Achiba, Y. *Z. Phys. D* **1997**, *40*, 414−417.
(49) Jakowski, J.; Irle, S.; Morokuma, K. *Phys. Chem. Chem. Phys.* **2012**, *14*, 6273−6279.